6th IEEE RAS/EMBS International Conference on
Biomedical Robotics and Biomechatronics (BioRob)
June 26-29, 2016. UTown, Singapore

Swimming Characteristics of Helical Microrobots in Fibrous Environments

Franziska Ullrich[1], Famin Qiu[1], Juho Pokki[1], Tianyun Huang[2], Salvador Pané[1] and Bradley J. Nelson[1]

***Abstract*— Wireless magnetic microrobots show great potential for targeted drug delivery or as minimally invasive surgical tools in the human body. In order to swim through bodily fluids, such as the vitreous humor in the eye, they must be equipped to successfully move through viscoelastic fluids, where they are obstructed by fibrous networks or microparticles. Prior researchers have shown an increased propulsion efficiency with increasing viscoelastic properties for artificial helical swimmers and bacteria with helical flagella. This work investigates the effect of solutions with increasing collagen concentrations on the propulsion velocity of a magnetically actuated helical microswimmer. Results are in agreement with prior experiments and theory and show a performance peak for a helical microrobot of length 280 μm swimming in a fibrous solution with collagen concentration of 1578 μg/ml.**

I. INTRODUCTION

Untethered magnetic microrobots show great potential to be used in targeted drug delivery or minimally invasive surgery throughout the human body, as they can be guided wirelessly by external magnetic fields to a pathological site [1], [2]. In order to function in the human body, microrobots must be equipped to swim through specific bodily fluids and propulsion is often obstructed by small structures in those fluids, such as fibres or microparticles. Many areas in the body exist where microrobots could be employed, such as the blood stream, the central nervous system (brain and spine), or the urinary tract [1]. One organ with high potential for microrobotic surgery is the posterior eye [2], [3], where the wireless microrobot must swim through vitreous humor. The vitreous humor is a viscoelastic fluid, containing a collagen fibre scaffold and water as a fluid solvent. The long, thin fibrils in the vitreous humor are typically $12 - 15$ nm in diameter and are mainly composed of three different collagen types (types II, IX and V/XI) [4]. To guide microrobots through the vitreous humor in the posterior eye, it is important to consider not only the macroscopic viscosity of the fluid, but also the interactions at the molecular and microstructural level [5], [6].

Magnetic helical microrobots, powered by external rotating magnetic fields, were first presented by Bell et al. in 2007 [7] and further characterised by Zhang et al. and Peyer et al. [8], [9], [10]. These microscopic helical swimmers are inspired by the corkscrew motion of bacteria flagella, such as *Escherichia coli* or *Borrelia burgdorferi*. They can perform 3-dimensional (3D) navigation in various liquids under low-strength rotating magnetic fields (<10 mT). Recently, nano-helices have been demonstrated to propel through human blood [11]. Other recent studies have shown that they can be used for single-cell targeted drug delivery *in vitro* [12], [13], [14] and can be wirelessly actuated *in vivo* [15]. Resistive-force theory (RFT) of flagellar propulsion is commonly used for hydrodynamic analysis of swimming flagella and was originally proposed by Gray and Hancock [16], [17]. The theory was first applied to flagellated bacteria [18], predicting a decrease in swimming velocity with increasing viscosity of the environment. However, the flow field created by a helical swimmer in a viscoelastic medium is described by a complex and highly nonlinear system. Many parameters influence the flow field, such as additional polymeric stresses created by the flow field, the response of the flow field to the polymeric stresses, and the interaction of solvent and polymeric forces with the helix [19]. Berg and Turner have shown that helically shaped bacteria, such as *Leptospira* or *Escherichia coli*, can exploit the fibre structures inside a viscoelastic fluid and swim more rapidly in methylcellulose than in nonviscoelastic solutions. The higher swimming efficiency is due to the fibre network exerting forces normal to a segment of the helix and the helical organism can *push* itself forward, increasing the effective pitch of the helical motion [20]. These bacteria are small enough to swim through the empty spaces of a structured fibre network and thus, feel the microscopic

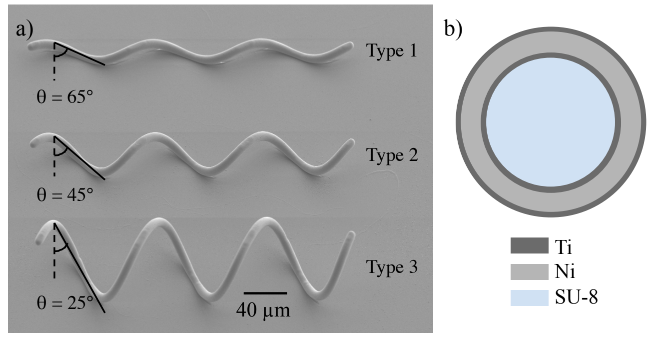

Fig. 1. a) Scanning electron microscope image of three types of helical microrobots with helical angles of 65°, 45° and 25°. All three types have a length of 280 μm. In this study, type 2 is utilised for all experiments. b) Cross-section of a helical microrobot showing layers of Ti, Ni and SU-8.

*This work was not supported by any organization

[1]Franziska Ullrich, Famin Qiu, Juho Pokki, Salvador Pané and Bradley J. Nelson are with the Multi-Scale Robotics Lab, ETH Zurich, Tannenstrasse 3, 8092 Zurich, Switzerland. fullrich@ethz.ch, famin.qiu@gmail.com, juho.pokki@gmail.com, vidalp@ethz.ch, bnelson@ethz.ch

[2]Tianyun Huang is with the University of Science and Technology Liaoning, Qianshanzhonglu 185, 114044, Anshan, Liaoning, China. ty_huang3@hotmail.com

viscosity of the solvent rather than the macroscopic viscosity of the solution. Magariyama and Kudo derived a model based on RFT to explain the increased swimming velocity of helices in fibrous environments. The model suggests that the fibre network forms a virtual tube around the thin-filament of the bacterium and allows it to enhance propulsion in the tube resulting in movement that is similar to corkscrew motion in solid matter without slippage [21]. However, the model assumes that the thickness of the filament is smaller than the space between the fibres in the network. Leshansky proposes a model that assumes sparsely distributed spherical particles instead of fibres in the fluid. The model suggests an increasing effective pitch of the helical swimmer due to the particles in the fluid without restrictions on filament thickness [22].

Many researches have experimentally confirmed the mathematical models of increased propulsion efficiency with increasing viscoelasticity. Liu et al. [23] studied the force-free swimming speed of a rotating helix in viscoelastic Boger fluid and conclude that swimming speed can decrease or increase as a function of the geometry of the swimming waveform and the Deborah number, which characterises the fluidity of the surrounding solution. A numerical study of helical swimming in an Oldroyd-B fluid model has shown that beyond a critical pitch angle of the helix with different filament sizes a range of Deborah numbers can be found for which swimming speed is higher than in a nonviscoelastic Newtonian fluid [19]. The increase of swimming velocity due to increased fibre concentration in a medium is explained mathematically due to boundary conditions at the structure-fluid interface by Fu et al. [24]. For a sparse fibre network, the helical swimmer does not exert force directly on the network. Instead forces are mediated through the solvent and network traction vanishes. In a dense fibre network, the swimmer is in direct contact with the fibres, causing stress in the network. Schamel et al. succeeded in propelling magnetically actuated nano-sized swimmers through a fibrous hyaluronan solution. The proposed nanoscrew has a length of $400\,\mathrm{nm}$ and displays enhanced propulsion velocities in fibrous solutions, while it cannot swim in pure water due to Brownian motion [25].

Most experimental studies focus on the swimming speed of real biological structures, thus generalisation of the results are limited due to variability and complexity of individual swimmers. However, theoretical explanations of swimming behaviour of helical structures assume idealised models. In this work, we investigate the swimming behaviour of magnetically actuated helical microswimmers in solutions with various collagen fibre concentrations as a model for the human vitreous humor. Results are in agreement with prior research showing increased propulsion properties for higher fibre content.

II. HELICAL MICROROBOTS

The geometry of the helical microrobot is inspired by the helical tail of bacteria, such as *Escherichia coli* or *Borrelia burgdorferi*. The size and shape are determined by several parameters, namely the helical angle θ, the total length of the helical swimmer, and the geometry of the filament, as illustrated in Fig. 1a).

The helical microrobots consist of a helical body made from SU-8 polymer and a nickel (Ni) and titanium (Ti) bi-layer around the body, as depicted in Fig. 1b). The movement of the helical microrobot is controlled by external rotating magnetic fields. As the unifom magnetic field rotates, thus applying a magnetic torque τ, the device is rotated about its helical axis. The forward motion of the helical structure is caused by the non-reciprocal corkscrew motion in a low Reynolds number regime. The maximum rotational speed of the device, or step-out frequency ω_{max}, depends on the applied magnetic torque τ_{max}, as in

$$\omega_{max} = \frac{a}{ac - b^2} \cdot \tau_{max}, \tag{1}$$

where a, b and c correspond to geometrical coefficients of the helical structure [26]. At its step-out frequency, the helical structure is no longer able to follow the rotation of the field and slows down. The maximum velocity u_{max} depends on the step-out frequency as described by

$$u_{max} = -\frac{b}{a} \cdot \omega_{max} = \frac{b}{b^2 - ac} \cdot \tau_{max} \tag{2}$$

For Newtonian fluids the velocity u_{max} is independent of the viscosity, whereas the fibres in a fibrous solution can change the drag on the helical structure in an inhomogeneous way. This can lead to different apparent viscosities in the coefficients a, b and c [5], [21].

III. PRELIMINARY STUDIES

A preliminary study investigated swimming qualities of three helical structures, as illustrated in Fig. 1a), named types 1, 2 and 3. The overall lengths of all three types is the same (280 μm), while the helical angles θ differ, as shown on the figure. Tests were performed with the structures swimming in water and two types of silicone oil with kinematic viscosities $350\,\mathrm{mm^2/s}$ and $1000\,\mathrm{mm^2/s}$, respectively. The maximum swimming velocities were measured and showed that helical structure type 2 (with a helical angle of $\theta = 45°$) is the fastest of the tested types. This finding is also confirmed in [22], where the best propulsion efficiency is mathematically derived at a helical angle of $45°$ for all values of hydrodynamic resistance. Thus, in this work, the type 2 structure was used for all experiments.

IV. MATERIALS AND METHODS

A. Microrobot Fabrication

A layer with thickness of $100\,\mu\mathrm{m}$ of SU-8 50 photoresist (Microchem) was first spin-coated on a glass substrate at $1000\,\mathrm{rpm}$ for $30\,\mathrm{s}$ followed by a soft bake process using a hot plate at 65 °C for 10 min and 95 °C for 30 min. The 3D helical microstructures were then written in the photoresists using 3D Direct Laser Writing [27] (Photonic Professional laser lithography system, Nanoscribe GmbH) with the oil-immersion 63× objective. The laser power and scan speed were set to 6.8 mW and 50 μm/s. After a post exposure bake, the substrate was developed in 1-methoxy-2-propanol-acetate (PGMEA) for 19 min and rinsed with isopropyl alcohol (IPA). The substrate was then dried with nitrogen gas. The developed glass substrates were evaporated with Ti/Ni/Ti (20 nm / 400 nm / 5 nm) multilayers by an electron beam evaporator (Plassys-II MEB550SL) with a rotational speed of 4 rpm, and tilt angle of 15°. The deposition rate of Ni and Ti films was 0.2 nm/s.

B. Collagen Solution Preparation

To model the helical swimmer contact with vitreous humor, gelatin that consists of several types of collagen was used [28], [29]. Six aqueous solutions of gelatin with different concentrations (350, 502, 974, 1578 and 2480 μg/mL) were prepared to investigate the helical microrobot's swimming behaviour. To prepare the solutions, gelatin (Sigma-Aldrich, CAS 9000-70-8, SKU 48723) was first weighed in a glass container. The container was then filled with 35 mL of water preheated to 60 °C to guarantee a temperature higher than the gelatin melting point at around 35 °C. The container was then closed with a cap, mixed with a vortex mixer at >1000 rpm and kept on a hotplate to maintain its temperature for 20 min. Afterwards, the solutions were mixed again with a vortex mixer (>1000 rpm) and placed in a refrigerator at 5 °C for >3 h to allow for stabilisation during the gelation process. Control solutions with pure deionized water (noted as 0 μg/mL gelatin) were also used for experiments. For best results, swimming experiments were conducted between two and 24 hours after solution preparation. Viscosity and temperature measurements were performed both before and after every experiment session. Viscosity was measured using a viscometer (custom-made by Rheonics, Zurich, Switzerland) and temperature was measured using a thermocouple (K type).

C. Electromagnetic Setup

The helical microrobots were actuated by uniform rotating magnetic fields that were generated by a Helmholtz coil setup consisting of three orthogonal coil pairs (Fig. 2). The system creates a rotating magnetic field $\overrightarrow{B}$ and induces a torque $\overrightarrow{T}$ that acts to align the microrobot's magnetisation $\overrightarrow{M}$ with the magnetic field as in

$$\overrightarrow{T} = v \cdot \overrightarrow{M} \times \overrightarrow{B} \tag{3}$$

where v is the magnetic volume of the microrobot. The helical swimmer's orientation is described with yaw and pitch values, the orientation parameters of the swimmer in and out of the horizontal plane, respectively. The custom software controls four independent parameters, *i.e.* the magnetic field strength, the rotational frequency of the field, and the orientation parameters yaw and pitch [30]. The applied frequencies in this study (<50 Hz) are well below the maximum frequencies that can be generated by the system. The movement of the helical swimmer was recorded with a camera through a microscope (Fig. 2a).

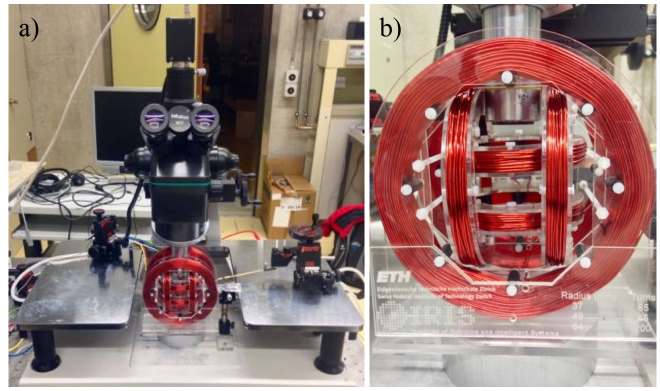

Fig. 2. Electromagnetic hardware setup (a) for manipulation of helical microrobots, including three Helmholtz coil pairs (b) and a microscope and camera for observation of the workspace.

TABLE I
VISCOSITY MEASUREMENTS OF THE VARIOUS GELATIN SOLUTIONS PRE AND POST THE EXPERIMENTAL PROCEDURE AT 24 °C.

Concentration	pre (Pas)	post (Pas)
0 μg/mL	1.000	1.000
350 μg/mL	1.016	1.018
502 μg/mL	1.022	1.005
974 μg/mL	1.081	1.090
1578 μg/mL	1.102	1.130
2480 μg/mL	1.130	1.147

D. Experimental Procedure

Prior to experimentation the wafer, which contains the fabricated helical structures, was cleaned thoroughly by first emerging it in acetone and then placing it in an ultrasonic bath for 5 min. This cleaning process was repeated with isopropyl alcohol and deionized water. For experimentation the fabrication wafer was placed in a container that was filled with the gelatin solution and then placed in the central workspace of the electromagnetic system. A manually controlled tungsten tip was used to transfer a helical swimmer from the fabrication wafer to the swimming area where it was submerged in the gelatin solution. The helical swimmer was moved by incrementally increasing the rotation frequency of the rotating magnetic field, while maintaining the swimmer's orientation constant. Images of the motion and corresponding field strengths and rotational frequencies were recorded for post-processing. During post-analysis a Matlab program tracks the swimmer on the recorded images and allows for the analysis of forward and drift velocities of a swimmer.

V. RESULTS

The viscosity and temperature of each gelatin solution are measured before and after the experimental procedure. All measured temperatures are 24 °C. Table I summarises the results for viscosity measurements for various collagen fibre

TABLE II
AVERAGE MAXIMUM VELOCITIES AND STANDARD DEVIATIONS, MEASURED AT DIFFERENT MAGNETIC FIELD STRENGTHS AND VARIOUS GELATIN CONCENTRATIONS.

Concentration	3 mT	6 mT	9 mT
0 μg/mL	812 ± 61 μm/s	1297 ± 330 μm/s	2138 ± 233 μm/s
350 μg/mL	30 ± 4 μm/s	174 ± 127 μm/s	338 ± 116 μm/s
502 μg/mL	174 ± 263 μm/s	109 ± 150 μm/s	13 ± 10 μm/s
974 μg/mL	48 ± 43 μm/s	13 ± 9 μm/s	34 ± 34 μm/s
1578 μg/mL	407 ± 265 μm/s	1013 ± 405 μm/s	1888 ± 103 μm/s
2480 μg/mL	3 ± 1 μm/s	24 ± 18 μm/s	142 ± 81 μm/s

concentrations. The motion of a helical swimmer in gelatin of concentration $1578\ \mu g/mL$, including time and rotational frequency, is shown in the supplementary materials.

The forward velocity of each helical structure is measured and plotted against the corresponding rotational frequency of the magnetic field. The magnetic field strength and collagen concentration are reported for each sample. An example plot is shown in Fig. 3. The figure shows three velocity measurements, executed with three different helical structures actuated in water with a magnetic field strength of $3\ \mathrm{mT}$. The mean and standard deviation of the forward velocities are calculated at each measured frequency. The region, labelled *A* on the plot, shows a gradual increase of the structure's forward velocity with increasing rotational frequency until the step-out frequency is reached at point *B*, where a large drop of the forward velocities is recorded (labelled *C*).

Figure 4 illustrates the mean measured forward velocity at various frequencies of the rotating magnetic field with a magnitude of $9\ \mathrm{mT}$ for helical swimmers actuated in different gelatin concentrations. The maximum forward velocities are measured and plotted against gelatin concentration for magnetic field strengths of 3, 6 and $9\ \mathrm{mT}$ in Fig. 5. The average maximum velocities of measured helical structures in various concentrated gelatin solutions are summarised in Tab. II for the three magnetic field strengths. The corresponding step-out frequencies are summarised in Table III.

TABLE III
AVERAGE STEP-OUT FREQUENCIES, MEASURED AT DIFFERENT MAGNETIC FIELD STRENGTHS AND VARIOUS GELATIN CONCENTRATIONS.

Concentration	3 mT	6 mT	9 mT
0 μg/mL	14 Hz	22 Hz	26 Hz
350 μg/mL	2 Hz	4 Hz	16 Hz
502 μg/mL	2 Hz	4 Hz	4 Hz
974 μg/mL	2 Hz	2 Hz	6 Hz
1578 μg/mL	14 Hz	16 Hz	32 Hz
2480 μg/mL	8 Hz	10 Hz	8 Hz

VI. DISCUSSION

This study investigates the swimming performance of helical microstructures in fibrous environments with different collagen fibre concentrations. As described in Eq. 1 and 2, it is observed that maximum velocity and step-out frequency positively correlate with increasing magnitude of the external rotating magnetic field, due to increasing magnetic torques. Viscosity measurements before and after experiments (Tab. I) show a slight increase in macroscopic viscosity of the solutions. Presumably, gelation continues during the experimental process, but the measured increase is negligible.

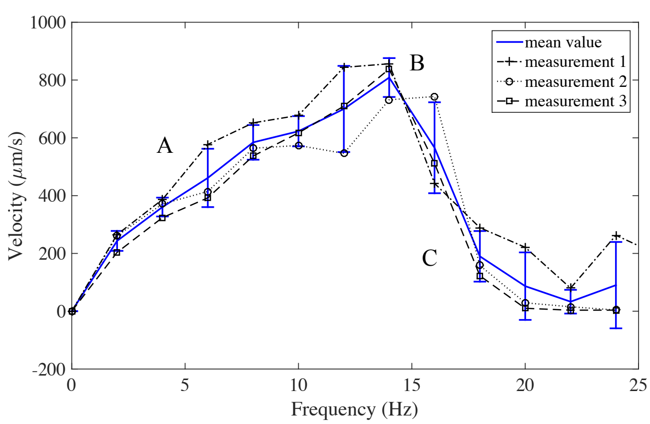

Fig. 3. Measured velocity of helical swimmer measured at various frequencies of the rotational magnetic field at magnetic field strength of $3\ \mathrm{mT}$ in water.

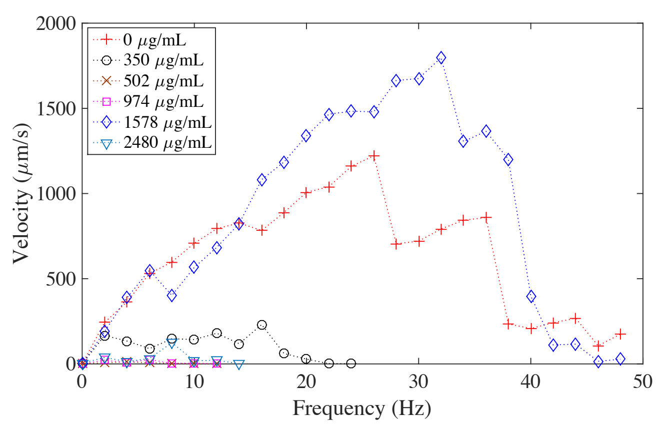

Fig. 4. Mean maximum velocities, measured at magnetic field strength of $9\ \mathrm{mT}$ and various gelatin concentrations. Measurements were performed with frequencies between 0 and 48 Hz.

Results suggest that it becomes more difficult for the helical structures to move in fibrous media compared to pure water as the maximum velocity and step-out frequency decrease. The structures swim freely in a solution with collagen fibre concentration of $0\ \mu g/mL$ (pure water) and performance quickly declines after introduction of collagen fibres to the solution. A performance peak is observed for helical swimmers in a gelatin solution with a concentration of $1578\ \mu g/mL$ for all measured magnetic field magnitudes, namely 3, 6 and $9\ mT$. The most notable performance peak occurs at $9\ mT$ where the measured maximum velocity is higher than that in water. If collagen fibre concentration is increased further, performance drops and the helical microrobot's movement becomes essentially zero.

The enhanced swimming performance of the helical microrobot at gelatin concentration of $1578\ \mu g/mL$ is illustrated in Fig 5. These findings corresponds to the experimental evidence of increased swimming speed of bacteria in fibrous environments observed by Berg and Turner [20]. Our observations are also in agreement with the mathematical model of Magariyama et al. [21] that describes increased swimming efficiency in fibrous fluids. As described by Pelc et al. [31], at low gelatin concentrations agglomerates of collagen are formed which could act as obstacles for the helical swimmer, decreasing the propulsion velocity compared to that in pure water, where no obstacles are present. Increasing the concentration of gelatin triggers the gelation process and a fibre network is formed, which according to theory [20], [21] increases the helical swimmer's velocity. Above a critical concentration of gelatin, an increasing amount of collagen-type triple helices are formed that could act as obstacles or become entangled in the helical swimmer and decrease its propulsion velocity. This possible explanation for the helical swimmer's measured propulsion velocity profile (Fig. 5) is depicted in Fig. 6.

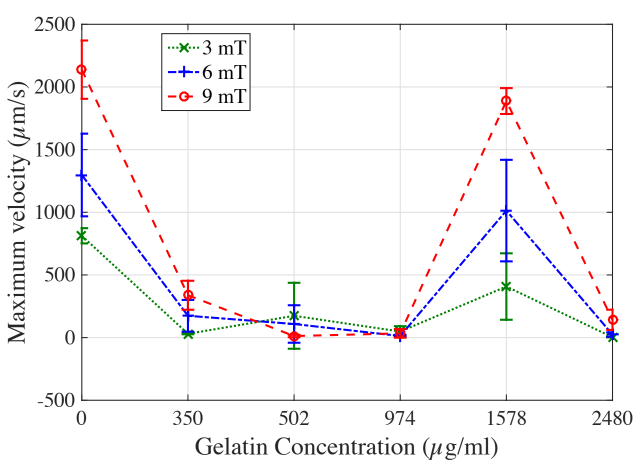

Fig. 5. Mean and standard deviation of measured maximum velocities of helical swimmers in various gelatin concentrations and with magnetic field strengths of 3, 6 and $9\ mT$.

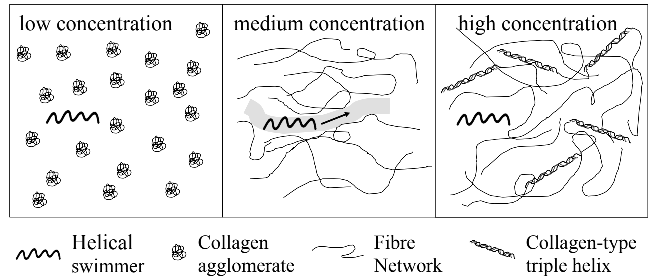

Fig. 6. At low gelatin concentrations collagen forms agglomerates, which constrain swimmer propulsion. According to theory [20], [21], at medium concentrations, a "virtual tube" forms in the collagen fibre network which enhances swimmer velocity. At high gelatin concentrations increasing amounts of collagen-type triple helices form that might obstruct swimmer propulsion [31].

The presented results are derived in vitreous humor phantoms with a range of collagen fibre concentrations, representing the changing configuration of the human vitreous humor due to ageing [32]. The results, illustrated in Fig. 5, suggest that the geometry of an intravitreal helical structure must be configured according to the surrounding fibre concentration for efficient swimming.

VII. CONCLUSION

This work investigates the swimming performance of helical microrobots in fibrous environments with various collagen fibre concentrations. Results show a general decrease of swimming quality, characterised by maximum swimming velocity and step-out frequency, with decreasing magnetic field strength. Propulsion efficiency is generally higher in water than in the fibrous solution. However, it is observed that movement is enhanced by the presence of collagen fibres at a gelatin concentration of $1578\ \mu g/mL$. This behaviour corresponds to the experimental findings of Berg and Turner [20] who observed increasing swimming efficiency of bacteria in fibrous fluids. Our findings are also in agreement with the mathematical model of Magariyama et al. [21] that describes enhanced propulsion of helical swimmers in fibrous environments due movement similar to corkscrew motion without slippage.

To confirm our findings, future work will focus on performing a larger number of measurements that analyse swimming properties of helical microrobots in solutions with various gelatin concentrations and gelatin strengths. We will also investigate the statistical relevance of our findings. More experiments will be performed between gelatin concentrations $974\ \mu g/mL$ and $2480\ \mu g/mL$ to characterise the velocity peak in more detail.

ACKNOWLEDGMENT

This work was supported by the European Research Council Advanced Grant BOTMED.

References

[1] B.J. Nelson, I.K. Kaliakatsos, J.J. Abbott, *Microrobots for minimally invasive medicine*, Annu. Rev. Biomed. Eng. vol. 12, pp. 55-85, 2010.

[2] F. Ullrich, C. Bergeles, J. Pokki, O. Ergeneman, S. Erni, G. Chatzipirpiridis, S. Pané, C. Framme, B.J. Nelson, *Mobility Experiments With Microrobots for Minimally Invasive Intraocular SurgeryMicrorobot Experiments for Intraocular Surgery*, IOVS, vol. 54(4), pp. 2853-2863, 2013.

[3] C. Bergeles, M.P. Kummer, B.E. Kratochvil, C. Framme, B.J. Nelson, *Steerable intravitreal inserts for drug delivery: in vitro and ex vivo mobility experiments*, MICCAI, pp. 33-40, 2011.

[4] P.N. Bishop, M. Takanosu, M. Le Goff, R. Mayne, *The role of the posterior ciliary body in the biosynthesis of vitreous humour*, Eye, vol. 16(4), pp. 454-460, 2002.

[5] K.E. Peyer, F. Qiu, L. Zhang, B.J. Nelson, *Movement of artificial bacterial flagella in heterogeneous viscous environments at the microscale*, IROS, pp. 2553-2558, 2012.

[6] B.J. Nelson, K.E. Peyer, *Micro- and Nanorobots Swimming in Heterogeneous Liquids*, ACS Nano, vol. 8(9), pp. 8718-8724, 2014.

[7] D.J. Bell, S. Leutenegger, K.M. Hammar, L.X. Dong, B.J. Nelson, *Flagella-like propulsion for microrobots using a nanocoil and a rotating electromagnetic field*, ICRA, pp. 1128-1133, 2007.

[8] L. Zhang, J.J. Abbott, L. Dong, K.E. Peyer, B.E. Kratochvil, H. Zhang, C. Bergeles, B.J. Nelson, *Characterizing the swimming properties of artificial bacterial flagella*, Nano Letters, vol. 9(10), pp. 3663-3667, 2009.

[9] L. Zhang, J.J. Abbott, L. Dong, B.E. Kratochvil,D.J. Bell, B.J. Nelson, *Artificial bacterial flagella: Fabrication and magnetic control*, Applied Physics Letters, vol. 94(6), pp. 064107, 2009.

[10] K.E. Peyer, L. Zhang, B.J. Nelson, *Bio-inspired magnetic swimming microrobots for biomedical applications*, Nanoscale, vol. 5(4), pp. 1259-72, 2013.

[11] P.L. Venugopalan, R. Ranajit, Y. Chandorkar, B. Basu, S. Shivashankar, A. Ghosh, *Conformal Cytocompatible Ferrite Coatings Facilitate the Realization of a Nanovoyager in Human Blood*, Nano Lett., vol. 14(4), pp. 1968-1975, 2014.

[12] F. Qiu, R. Mhanna, L. Zhang, Y. Ding, S. Fujita, and B.J. Nelson, *Artificial bacterial flagella functionalized with temperature-sensitive liposomes for controlled release*, Sensors and Actuators B: Chemical, vol. 196, pp. 676-681, 2014.

[13] R. Mhanna, F. Qiu, L. Zhang, Y. Ding, K. Sugihara, M. Zenobi-Wong, et al., *Artificial Bacterial Flagella for Remote-Controlled Targeted Single-Cell Drug Delivery*, Small, vol. 10, pp. 1953-1957, 2014.

[14] F. Qiu, S. Fujita, R. Mhanna, L. Zhang, B.R. Simona, and B.J. Nelson, *Magnetic Helical Microswimmers Functionalized with Lipoplexes for Targeted Gene Delivery*, Advanced Functional Materials, vol. 25, pp. 1666-1671, 2015.

[15] S. Ania, F. Qiu, M. Mazza, K. Kostarelos, and B.J. Nelson, *Controlled In Vivo Swimming of a Swarm of Bacteria-Like Microrobotic Flagella*, Advanced Materials, vol. 27, pp. 2981-2988, 2015.

[16] J. Gray, G.J. Hancock, *The propulsion of sea-urchin spermatozoa*, J. Exp. Biol., vol. 32(4), pp. 802-814, 1955.

[17] S. Childress, *Mechanics of swimming and flying*, 2nd ed., Cambridge University Press, 1981.

[18] M.E. Holwill, R.E. Burge, *A hydrodynamic study of the motility of flagellated bacteria*, Arch. Biochem. Biophys., vol. 101, pp. 249-260, 1963.

[19] S.E. Spagnolie, B. Liu, T.R. Powers, *Locomotion of helical bodies in viscoelastic fluids: enhanced swimming at large helical amplitudes*, Physical Review Letters, vol. 111(6), pp. 068101, 2013.

[20] H.C. Berg, L. Turner, *Movement of microorganisms in viscous environments*, Nature, vol. 278, pp. 349-351, 1979.

[21] Y. Magariyama, S. Kudo, *A Mathematical Explanation of an Increase in Bacterial Swimming Speed with Viscosity in Linear-Polymer Solutions*, Biophysical Journal, vol. 83(2), pp. 733-739, 2002.

[22] A.M. Leshansky, *Enhanced low-Reynolds-number propulsion in heterogeneous viscous environments*, Physical Review E, vol. 80(5), pp. 051911, 2009.

[23] B. Liu, T.R. Powers, K.S. Breuer, *Force-free swimming of a model helical flagellum in viscoelastic fluids*, PNAS, vol. 108(49), pp. 19516-19520, 2011.

[24] H.C. Fu, V.B. Shenoy, T.R. Powers, *Low-Reynolds-number swimming in gels*, EPL (Europhysics Letters), vol. 91(2), pp. 24002, 2010.

[25] D. Schamel, A.G. Mark, J.G. Gibbs, C. Miksch, K.I. Morozov, A.M. Leshansky, P. Fischer, *Nanopropellers and Their Actuation in Complex Viscoelastic Media*, ACS Nano, vol. 8(9), pp. 8794-8801, 2014.

[26] J.J. Abbott, K.E. Peyer, M.C. Lagomarsino, L. Zhang, L. Dong, I.K. Kaliakatsos, B.J. Nelson, *How should microrobots swim?*, Int. J. Robot. Res., vol. 28(11-12), pp. 1434-1447, 2009.

[27] S. Tottori, L. Zhang, F. Qiu, K.K. Krawczyk, A. Franco-Obregon, B.J. Nelson, *Magnetic Helical Micromachines: Fabrication, Controlled Swimming, and Cargo Transport*, Advanced Materials, vol. 24(6), pp. 811-16, 2012.

[28] S. Gorgieva and V. Kokol, *Collagen-vs. gelatine-based biomaterials and their biocompatibility: review and perspectives*, Biomaterials Applications for Nanomedicine, Ed. R. Pignatello, INTECH Open Access Publisher, 2011.

[29] M.A. Masuelli, M. G. Sansone, and D. F. Aplicada. *Hydrodynamic properties of gelatin-studies from intrinsic viscosity measurements*, Products and Applications of Biopolymers, Ed. C. J. R. Verbeek, INTECH Open Access Publisher, 2012.

[30] L. Zhang, K. Peyer, B.J. Nelson, *Artificial bacterial flagella for micromanipulation*, Lab Chip, vol. 10(17), pp 2203-2215, 2010.

[31] D. Pelc, S. Marion, M. Pozek, M. Basletic. *Role of microscopic phase separation in gelation of aqueous gelatin solutions*, Soft Matter, vol. 10, pp. 348-356, 2014.

[32] J. Sebag, *Ageing of the vitreous*, Eye, vol. 1, pp254-262, 1987.